The near-infrared spectra of the alkali carbonates

Laurence Hopkinson[a*], Ken J. Rutt[b], Petra Kristova[b]

[a] ([*]corresponding author)

[b] School of the Environment and Technology,

University of Brighton

Cockcroft Building, Lewes Road, Brighton.BN2 4GJ.

United Kingdom.

Tel: +44 (0)1273 642239, Fax: +44 (0)1273 642285, e.mail: l.hopkinson@brighton.ac.uk

School of Pharmacy and Biomolecular Sciences,

University of Brighton.

Huxley Building, Lewes Road, Brighton.BN2 4GJ.

United Kingdom.

Tel: +44 (0)1273 642076, Fax: +44 (0)1273 642285, e.mail: k.j.rutt@brighton.ac.uk

Tel: +44 (0)1273 642065, Fax: +44 (0)1273 642285, e.mail: p.kristova@brighton.ac.uk

Key words: alkali carbonates, overtones, combinations, vibration, libration.

Abstract

This study presents the first account of the near-infrared (NIR) spectra of the alkali carbonates: [Cs_2CO_3] [Rb_2CO_3] [K_2CO_3] [Na_2CO_3] and [Li_2CO_3]. Seven NIR bands (labelled [A] to [G] inclusive) within the [4000-6000cm^{-1}] (2.5 – 1.66μm) region of interest are common to the five spectra examined, of which six bands [A-C] and [E-G] proved amenable to quantitative study. The first three occur in the range 4067-4493cm^{-1} (2.458-2.226μm) and are assigned to a [CO_3^{2-}] $3\nu_3$ overtone, Bands [E] and [F] are centred at *ca* 4902cm^{-1} (2.04 μm) and *ca* 5034cm^{-1} (1.98 μm) respectively and are assigned to a ($2\nu_1 + 2\nu_3$) combination. Band [G] centred at *ca* 5190 cm^{-1} (1.92 μm) is assigned to a ($\nu_1 + 3\nu_3$) combination. One additional band (Band [X]) centred in the vicinity of *ca* 4080cm^{-1} (2.45μm) in all spectra other than [Cs_2CO_3] is assigned to ($2\nu_3 + 2\nu_4$). The data is compared with the corresponding additive sum of the mid-infrared (MIR) fundamental, or in the case of combinations, Raman and MIR fundamentals. The quantified differences between NIR band frequency and that of the corresponding MIR derived overtone or combination in the case of [Li_2CO_3] and [Rb_2CO_3] closely coincide with Raman active lattice modes of rotary origin. From which it is argued that vibration - libration combinations may operate across a range of NIR frequencies for these mineral types. NIR data from [K_2CO_3], [Cs_2CO_3] and [Na_2CO_3] are discussed in the light of these findings. The influences of differences in atomic mass and space group effects on the NIR spectra of the alkali carbonates are also demonstrated.

1. Introduction

Anhydrous carbonates number sixty-five mineral types in which the [CO_3^{2-}] radical provides all the negative charge [1]. The group 1 alkali metal carbonates ([Li_2CO_3], [Na_2CO_3], [K_2CO_3], [Rb_2CO_3] and [Cs_2CO_3]) constitute an important group of minerals which find application in a range of chemical processes [2]. All alkali carbonates are highly hygroscopic and water soluble [3]. The alkali carbonates have been investigated in a number of studies [4 - 8]. It is established that three types of anhydrous alkali carbonate mineral structures exist: [Li_2CO_3] (space group C2/c); [Na_2CO_3] (space group c2/m); and [K_2CO_3] (space group $p2_1/c$). The potassium carbonate is isostructural with [Rb_2CO_3] and [Cs_2CO_3] [4-7].

In common with other carbonate mineral groups [9,10] the [CO_3^{2-}] internal modes occur across a range of mid-infrared (MIR) wavenumber intervals (table 1). The Raman active v_1 (totally symmetric C-O stretching mode) appears at *ca* 1080cm^{-1}, the MIR active v_2 (out-of-plane bending mode) occurs at *ca* 880cm^{-1}, the MIR and Raman active v_3 doubly degenerate (anti-symmetric stretching mode) occurs around *ca* 1430cm^{-1}, while the doubly degenerate v_4 in-plane bending mode occurs around 715cm^{-1}. The v_4 internal mode is split in all of the alkali carbonates [4-7]. In the case of [Li_2CO_3] and the isostructural carbonates the remaining internal modes of the carbonate ion (v_1, v_2 and v_3) occur as single bands. The exception is [Na_2CO_3] which displays a doublet structure for each of the internal modes (Table 1), interpreted in terms of two non-equivalent orientations of the [CO_3^{2-}] ion within the primitive unit cell [4,10].

For carbonate minerals the near-infrared region contains bands due to overtone and combination tones of the [CO_3^{2-}] anion, also where present evidence of [H_2O] [9]. However we can find no published accounts of the near-infrared spectra of any of the alkali carbonates although it seems certain that the differing crystal structures will find expression in the resultant spectra as will any evidence of hydration. Further, studies of other anhydrous carbonate mineral groups indicate that correlations between specific near-infrared wavelengths and different metal cations exist and that combinations between external (lattice) modes and the internal modes of molecular origin may exist [11]. To this end this study presents the near-infrared (NIR) spectra of the alkali carbonates and explores crystal chemical correlations between the spectra with Raman and MIR findings.

2. Materials and Methods

The powdered alkali metal carbonates examined in this study were sourced from international suppliers: lithium carbonate (Acros Organics, lot number (lot. n.) A0231490), sodium carbonate (Honeywell Fluka, lot. n. SLBQ8163V), potassium carbonate (Fisher Scientific, lot. n. 0886824), rubidium carbonate (Sigma Aldrich, lot.n. MKBW4880V) and cesium carbonate (Sigma Aldrich, lot.n. MKBZ2431V). Samples were oven-dried at 100°C for twenty four hours and immediately placed in a desiccator and then placed in the standard reflectance glass tubes supplied with the NIR instrument by Perkin Elmer. The tubes were filled 2cm deep with the powders. A small bag containing desiccant was placed on top of the sample before sealing the tube with a plastic stopper. The spectra were then measured immediately. Several repeat measurements were taken for each powder sample type. NIR analyses were conducted with a Perkin Elmer Spectrum 100N spectrometer. The powdered samples were measured at room temperature in the range 4000-10000cm^{-1}. The samples were measured using NIRA (near-infrared reflectance accessory) which is used to collect diffuse reflectance spectra of solids and powders. The measurements were done in absorbance.The NIR measurement protocol is as follows. A background scan is taken and a scan type is selected to be interleaved (i.e. the shuttle automatically moves to the rear position to take background scan before moving to the front position to scan the sample and display the ratioed sample spectrum). The number of scans collected was 8, resolution 16cm^{-1}, INGAAS detector selected, optical path difference velocity 1.00 cm/sec.

Raman analyses were performed with a Perkin Elmer Raman Identicheck fitted with a 785nm laser, a CCD detector and a fibre-optic probe with 70mW laser power. The probe spot size is 100µm, working distance is 7.5mm. The samples were measured in the spectral range 2000-100cm^{-1}, with 2cm^{-1} resolution. Each spectrum was collected from 8 scans for 2 seconds. Data manipulation was performed using the software Spectrum (Perkin Elmer) and PeakFit (Jandel, Scientific Software). First derivative (Gaussian) peak-fitting was employed on all spectroscopic data using Jandel Scientific PeakFit software. All values reported show $r^2 > 0.995$. All data was collected at the University of Brighton (United Kingdom).

3. Experimental results

3.1 The near-infrared spectra of the alkali carbonates

In common with all NIR spectra which emerge from overtones and combinations of fundamental MIR absorptions [12] the alkali carbonates show a range of broad variably resolved overlapping

bands in the [4000-6000cm^{-1}] region, which are qualitatively similar in appearance to those of the alkaline earths carbonates [9]. Figure 1 shows the spectra and associated Peak-Fit software results for the five alkali carbonate mineral powders examined. Bands [A] to [G] inclusive are common to the five spectra and are central to this study (table 2). Those bands which are not common to all spectra are labelled [V] to [Z] inclusive. Band [V] is singular to [Na_2CO_3]. Band [W] may fall below the lower wavenumber detection range for [Rb_2CO_3] and [Cs_2CO_3], is close to 4000cm^{-1} for [Na_2CO_3], at 4020cm^{-1} for [K_2CO_3] and 4022cm^{-1} for [Li_2CO_3]. Band [X] is absent from the [Cs_2CO_3] spectrum. Bands [Y] and [Y^1] are singular to [Rb_2CO_3]. Peak-Fit software identified an additional weak band (band [Z]) in the vicinity of 5490cm^{-1} [Li_2CO_3], 5232cm^{-1} [Rb_2CO_3] and 5210cm^{-1} [Cs_2CO_3]. In other spectra the band was too poorly resolved relative to background to accurately position or analyse (marked [Z*] on figure 1), as were variably resolved extremely broad bands in the 5500-5800cm^{-1} region (marked [Z^{1,2}*] on figure 1). Band(s) in the vicinity of *ca* 5260cm^{-1} (1.9µm) theoretically could originate at least in part from the combination of H-O-H band with the antisymmetric OH stretch [9]. However near-infrared spectra do not show an accompanying asymmetric OH stretch at 7140cm^{-1} (1.49µm). Hence all bands listed in table 2 and displayed in figure 1 are interpreted as [CO_3^{2-}] radical-related spectral features although bands [Z^{*1,2}] proved too poorly resolved and broad in nature for meaningful quantitative study and are hereafter excluded from this study.

3.2 Bands [A] to [G], atomic mass and space group considerations

Figure 2 shows bands [A-G] inclusive plotted against the corresponding atomic mass (amu) of each co-ordinating cation. The figure shows that for each band [Na_2CO_3] occurs at higher wavenumbers than [Li_2CO_3]. Bands [A-C] and [E-G] show reasonable r^2 power-trend type fits for the isostructural carbonates with [Cs_2CO_3] occurring at lower wavenumbers than [K_2CO_3] while the [Rb_2CO_3] wavenumber values are intermediate with respect to [K_2CO_3] and [Cs_2CO_3]. Similar 'mass effects' on fundamental vibrations of internal modes in other carbonate mineral types have been assigned to small changes in the bending and stretching force constants, reflecting differences in the chemical bonding of the carbonate ion [10]. It is also evident from figure 2 that the relationship between increasing atomic mass and decreasing wavenumber does extend to [Na_2CO_3] and [Li_2CO_3] i.e. the [Na_2CO_3] bands occur at marginally higher wavenumbers than those of the [Li_2CO_3] powders, consistent with differing space group effects also exerting influence on band wavenumber positions.

In contrast to bands [A-C] and [E-G] band [D] shows no correlation between wavenumber and atomic mass for the isostructural carbonates. The reason for the singular absence of any correlation

is unclear. However, the spectrum of [Rb_2CO_3] shows a shoulder to band [D], marked [Y] and [Y^1] on figure 1. Hence, it is possible that band [D] in at least some of the other spectra is composite in nature but have gone either unresolved or partially resolved with Peak-Fit software, thereby accounting for the seemingly random nature of band [D] data. For this reason band [D] is not considered further in this study.

3.3 Band assignments [A-C]

In order to investigate relationships between the NIR data with MIR fundamental vibrations experimental data were plotted against the additive sums of overtones and combinations derived from data listed in table 1. For example, for each alkali carbonate the v_3 frequency listed in table 1 was multiplied by three to yield the overtone denoted M($3v_3$) etc. For [Na_2CO_3] in which each fundamental appears twice (with a small wavenumber separation between each) the average of the two band wavenumbers for each fundamental were taken (table 1).

In utilizing the MIR internal mode data it is important to note that the degenerate v_3 fundamental of carbonate minerals measured from powders are broad in MIR spectra with the measured wavenumber falling somewhere between the transverse and longitudinal components of v_3. Consequently measurements are generally considered less accurate than for other fundamentals. In the case of powdered calcite, a (± 12.5cm^{-1}) variation in the frequency of v_3 has been reported from seven separate studies [10]. Nevertheless, previous studies have successfully employed the infrared-active component of v_3 to document linear trends in a range of carbonate mineral compounds [13].

In comparison with the NIR spectra of other carbonate mineral groups [9] bands [A-C] occur across a wavenumber interval consistent with a [CO_3^{2-}] $3v_3$ overtone. Figure 3a shows the NIR data for bands [A-C] plotted against M($3v_3$). Band [A] [Cs_2CO_3], [Rb_2CO_3] and [Li_2CO_3] data are marginally lower than the corresponding M($3v_3$) values. Band [A] [K_2CO_3] data plus all band [B] and [C] data are greater than M($3v_3$). The three isostructural carbonates show linear trends of increasing wavenumber in the general order [K_2CO_3] > [Rb_2CO_3] > [Cs_2CO_3]. The best-fit trend tie-lines for bands [A], [B] and [C] are all angled oblique to the tie line linking the M($3v_3$) data points. The quantified number (cm^{-1}) to which separate NIR band data points deviate from M($3v_3$) wavenumber are given in figure 3a.

3.4 Band assignments [E-F]

Bands [E] and [F] are centred at *ca* 4902cm^{-1} (2.04 μm) and *ca* 5034cm^{-1} (1.98 μm) respectively (fig. 1). The wavelength intervals are both consistent with a ($2\nu_1 + 2\nu_3$) combination band [9]. Figure 3b shows bands [E] and [F] plotted against the corresponding additive sum M($2\nu_1 + 2\nu_3$). In common with bands [A],[B] and [C] the isostructural carbonates in bands [E] and [F] show increase in wavenumber [K_2CO_3] > [Rb_2CO_3] > [Cs_2CO_3]. For both bands the projected tie-lines linking the data points are oblique to the tie-line linking M($2\nu_1 + 2\nu_3$) data points. Band [E] [Na_2CO_3] data point closely coincides with the corresponding M($2\nu_1 + 2\nu_3$) value, whereas [Li_2CO_3] is offset 90cm^{-1} from its corresponding M($2\nu_1 + 2\nu_3$) total. All band [F] data exhibits NIR wavenumbers greater than M($2\nu_1 + 2\nu_3$). The greatest offset (167cm^{-1}) is shown by [K_2CO_3]. Conversely [Li_2CO_3] is practically coincident with its corresponding M($2\nu_1 + 2\nu_3$) total. Also plotted on figure 3b is the band [V] data point for [Na_2CO_3], which is offset 207cm^{-1} wavenumbers from the corresponding M($2\nu_1 + 2\nu_3$) total.

3.5 Band assignment [G]

Band [G] is centred at *ca* 5190 cm^{-1} (1.92 μm) (fig.1), consistent with a ($\nu_1 + 3\nu_3$) assignment [9]. All band [G] NIR data plots at lower wavenumbers than the corresponding M($\nu_1 + 3\nu_3$) totals (Fig. 3c). The isostructural carbonates show the same sequential ordering of increasing NIR wavenumber as previously described for bands [A-C] and [E-F]. The tie-line connecting them is orientated at a low oblique angle or sub parallel to that connecting M($\nu_1 + 3\nu_3$) totals. The [Li_2CO_3] data point is made conspicuous by its 194cm^{-1} offset from its corresponding M($\nu_1 + 3\nu_3$) total.

3.6 Band assignment [X]

Band [X] is centred in the vicinity of *ca* 4080cm^{-1} (2.45μm) in all spectra other than [Cs_2CO_3] (fig.1). Because the wavenumber of band [X] decreases from [Li_2CO_3] (4140cm^{-1}) to 4007cm^{-1} for [Rb_2CO_3] it may follow that band [X] for [Cs_2CO_3] may occur at <4000cm^{-1}. The wavenumber interval of band [X] data is consistent with a ($2\nu_3 + 2\nu_4$) assignment [9]. Band [X] NIR data is plotted against M($2\nu_3 + 2\nu_4$) in figure 3d. All data plots at lower values than corresponding M($2\nu_3 + 2\nu_4$) totals.

4. Interpretation

It is well documented that overtones are the whole number multiples of the fundamentals only to a first approximation and, because of the anharmonicity of vibration overtones are usually less than the additive sum the fundamental frequency [14]. Thus, the presence of differences between the

NIR band data and additive sums of MIR vibration fundamentals is not striking in the sense that anharmonicity of vibration implies that it should be so. What is apparent is that individual NIR band data sets are either greater or less than the whole number additive sum of the assigned overtone / combination, or else contain data which is both greater and less than that of the assignment (fig. 3). Further, the NIR data for the isostructural carbonates is sequentially ordered with respect to atomic mass, while different space group effects evidently exert influence on [Na_2CO_3] and [Li_2CO_3] spectra (fig. 2).

It has been demonstrated that lattice modes of rotatory origin can combine with internal modes of molecular origin to shift the pure molecular vibrational transition to higher and or lower frequencies [15,16]. Figure 4 shows the Raman spectra of the five carbonate powders in the 100-300cm^{-1} lattice mode region. [Li_2CO_3] differs significantly from the other spectra by virtue of possessing sharp high intensity Raman bands which suggests a far higher degree of ordering than the other alkali carbonates [4,10]. In contrast the [Na_2CO_3] powder exhibits Raman bands which are broad and diffuse. This difference is interpreted to indicate that [Na_2CO_3] is far less well ordered [4]. Broadening of lattice modes provides evidence of translational disorder in the stacking of [CO_3^{2-}] ions [10]. The Raman spectra of the three isostructural carbonates are characterised by broad overlapping bands similar in appearance to [Na_2CO_3] (fig. 4). However the width of the room temperature lattice modes of [K_2CO_3] and [Rb_2CO_3] are ascribed to thermal broadening distinct from the true disordering of [Na_2CO_3] [5]. Presumably thermal broadening also exerts influence on [Cs_2CO_3] as its Raman spectrum is qualitatively similar to that of the other isostructural carbonates (fig. 4).

Selection rules indicate that for [Li_2CO_3] twenty one lattice modes are expected which involve motions of the anion and cation sub lattices [7], of these the [Li_2CO_3] Raman spectrum shows three distinct sharp high intensity bands at 194, 157 and 128cm^{-1} (fig.4) which are believed to result from rotary motion of the carbonate groups [4]. A fourth high intensity band situated at slightly less than 100cm^{-1} wavenumbers is suggested by the asymmetric rise in background intensity towards the 100cm^{-1} detection limit and is in keeping with reports of a lattice mode at 96cm^{-1} [4]. Also evident is an undocumented band at 103cm^{-1} which is presumably another lattice mode (fig. 4). The 194cm^{-1} difference between NIR band [G] [Li_2CO_3] data and the corresponding M(v_1 + 3v_3) total coincides precisely in wavenumber with that of a Raman active lattice mode. Band [C] 103cm^{-1} offset from M(3v_3) total coincides exactly with that of another lattice mode. Band [E] offset from M(2v_1 + 2v_3) total (90cm^{-1}) is six wavenumbers from another known lattice mode. Band [X] is offset 184cm^{-1} from

the ($2\nu_3 + 2\nu_4$) assignment MIR total, placing the data point 10cm^{-1} wavenumbers from the [Li_2CO_3] 194cm^{-1} lattice mode (fig.6) and 8cm^{-1} from a second (very weak) lattice mode calculated at 176cm^{-1} [8]. Given that no polarization dependence can be determined from powders, meaning that different lattice modes of similar wavenumber may appear as a single band [10] the [Li_2CO_3] data is interpreted to provide evidence that lattice modes of rotatory origin do combine with overtones and combinations of internal modes of molecular origin in the case of the [Li_2CO_3] powder.

Any search for evidence of lattice modes combining with internal modes of molecular origin within the NIR spectra of the remaining alkali carbonates is difficult. The structural disorder of [Na_2CO_3] means that Raman peak positions are likely to be less precise than for [Li_2CO_3], plus additive sums of the [Na_2CO_3] fundamentals are based on the average of each doubled fundamental wavenumber pair (table 1). Thermal broadening of the isostructural carbonates means that significant numbers of lattice modes are only resolved by Raman spectroscopy at very low temperature [5,7]. In addition the lattice modes of [K_2CO_3] and [Rb_2CO_3] have been described as exceptionally complicated because forty five lattice modes are allowed by C2h unit cell group selection rules [5]. Further, analytical constraints commonly mean that very few studies report lattice modes at <100cm^{-1} from mineral powders. This fact may explain why we could find no published accounts of [Rb_2CO_3] lattice modes at less than 75cm^{-1} wavenumbers and no documented accounts of [Na_2CO_3] lattice modes at less than 98cm^{-1} wavenumbers.

Table 3 shows the wavenumber differences between NIR data from the five alkali carbonate powders relative to each band's mid-infrared additive sum of the overtone or combination assignment, together with the closest published account of a lattice mode frequency. Boxes within the table shaded grey indicate the absence of published accounts of low wavenumber lattice modes. Of the remaining data points twenty of the twenty one data points fall within 11cm^{-1} of a known lattice mode frequency. The outlier is band [F] [Cs_2CO_3] (97cm^{-1}) which shows a 17cm^{-1} separation from the nearest known lattice mode frequency (table 3). However peak-fitting of the Raman spectrum of [Cs_2CO_3] suggests the presence of a strong (previously unreported) band at *ca* 101cm^{-1}, i.e. within 4cm^{-1} of the band [F] [Cs_2CO_3] data point (fig. 4). In addition the [Rb_2CO_3] band [X] 121cm^{-1} wavenumber difference with the corresponding M($2\nu_3 + 2\nu_4$) additive sum is close to a peak-fit resolved Raman band at 117cm^{-1} (fig. 4) i.e. within 4cm^{-1} of the band [X] data point. Further, band [F] and [C] [Rb_2CO_3] data also closely coincide with additional high intensity Raman bands (fig. 4), suggesting that there is some evidence of lattice modes combining with internal modes of molecular origin in [Rb_2CO_3]. Data from [Cs_2CO_3] and [K_2CO_3] are open to interpretation as is [Na_2CO_3]. In the

case of the sodium carbonate a Raman active lattice mode at *ca* 90cm^{-1} has been reported [4] which is broadly coincident with three NIR bands data points (table 3). Further, band [V] data which is singular to the [Na_2CO_3] powder coincides with a weak Raman active band (fig. 3). However further research is required to corroborate these findings, in this respect THz spectroscopy may hold future promise.

5. Conclusions

Previous work has demonstrated that the vibrational spectra of molecular crystals may comprise pure vibration transitions of molecular origin enveloped by vibration - libration combinations which can shade individual bands to a higher and or lower frequency than in the pure vibrational transition [15]. Further, it has been shown that high frequency overtone and combination bands in the 3000 cm^{-1} to 5000 cm^{-1} region of calcite register lattice modes combining with v_3 overtones [9,16]. Because the difference in wavenumber of four [Li_2CO_3] bands with a $3v_3$ overtone and three combinations (calculated as additive sum of the fundamentals involved) closely coincide with that of Raman active rotary lattice modes it is argued that vibration - libration combinations occur across a variety of NIR wavelengths in [Li_2CO_3] and [Rb_2CO_3] alkali carbonate spectra. It is also suggested that data presented here is at least in part qualitatively in keeping with vibration - libration combinations operating within the NIR spectra of other alkali carbonates across a range of frequencies.

Isostructural carbonate data from bands [A-C] and [E-G] repeatedly fall in a sequential ordered pattern of NIR wavenumber decreasing with increasing atomic mass from [K_2CO_3] to [Rb_2CO_3] to [Cs_2CO_3] (fig. 2). This trend closely resembles that observed from calcite and aragonite group mineral powders [11], in which compression of the carbonate ion by its packing increases with decreasing cation size. In this respect of note [K_2CO_3] data from bands [B,C] and [E,F] consistently show the greatest disparity from the corresponding additive sum of the vibration fundamentals relative to [Rb_2CO_3] and [Cs_2CO_3]. Given that the same quantified disparities closely match that of a lattice mode it appears conceivable that librational anharmonicity may increase as cation size decreases in these four NIR bands.

Acknowledgements

The University of Brighton is thanked for financial support. The reviewers are thanked for their input. The data and samples are archived at the University of Brighton.

References

[1] L.B. Railsback . Carbonates and Evaporites. 14 (1999) 1-20.

[2] C.F. Windisch, J.L. Cox, E.N. Greenwell. Spectrochim. Acta A53 (1997) 1981-1993.

[3] C.J.H Schutte, K. Buis (1961) Spectrochim. Acta A17 (1961) 921-924.

[4] M.H. Brooker, J.B. Bates. J. Chem. Phys. 54 (1971) 4788-4796.

[5] M.H. Brooker, J.B. Bates. Spectrochim. Acta 30A (1974) 2211-2220.

[6] Y. Hase. An. Acad. Brasil. 52 (1980) 520-525.

[7] M.H. Brooker, J. Wang J. (1992) Spectrochim. Acta 48A (1992) 999-1008.

[8] N. Koura, S. Kohara, K. Takeuchi, S. Takahashi, L.A. Curtiss, M. Grimsditch, M. Saboungi. J. Mol. Struct. 382, (1996) 163-169.

[9] G.R. Hunt, J.W. Salisbury. Mod. Geol. 2 (1971) 23-30.

[10] W.B. White (1974), Farmer V.C (ed) The infrared spectra of minerals. Mineral Soc. Monogr. 4 (chap. 12) (1974) 227-282.

[11] L. Hopkinson, K. Rutt. Spectrochim. Acta A162 (2016) 105-108.

[12] F. Westad, A. Schmidt, M. Kermit M (2008). J. Near-Infrared Spec. 16 (2008) 265-273.

[13] H.H. Adler, P.F. Kerr P.F. Am. Miner. 48 (1963) 124-137.

[14] M. Reichenbächer, J. Popp. Challenges in Molecular Structure Determination. Springer-Verlag Berlin Heidelberg (2012) DOI 10.1007/978-3-642-24390-5_2.

[15] R.M. Hexter, D.A. Dows. J. Chem. Phys. 25 (1956) 504-509.

[16] R.M. Hexter. Spectrochim. Acta 10 (1958) 281-290.

Captions

Table 1. The wavenumbers (cm^{-1}) of internal modes (Int.) of [CO_3^{2-}] in the alkali carbonates. The [Li_2CO_3] and [Na_2CO_3] data is from [4]. Note that the v_1 vibration of the sodium carbonate is split as are all v_4 measurements (given in brackets). The mean of the wavenumbers for each split fundamental were taken for each carbonate mineral type for the purposes of the present study. Note that the [Na_2CO_3] data for the v_3 internal mode (marked with an asterix *) were measured through thin films at 80K. The [K_2CO_3] and [Rb_2CO_3] data are from [5]. The [Cs_2CO_3] internal mode data is from [6].

Table 2. Near-infrared data for bands [A-G] inclusive, plotted as wavenumbers cm^{-1}. The wavelength range for each band is given in microns (μm) beneath the band label title.

Table 3. All lattice mode (L. mode) data marked with an asterix was acquired at 80K, all other data was acquired at room temperature. Data marked with a superscript ([a]) is from [8]. L. mode data marked ([b]) is from [5]. L. mode marked ([c]) is from [4]. L. mode data marked ([d]) is from [7].. No data is available for areas shaded grey.

Figure 1. Near-infrared absorption spectra of: [Li_2CO_3]; [Na_2CO_3]; [K_2CO_3]; [Rb_2CO_3]; and [Cs_2CO_3] with peak-fit overlays. See text for details**.**

Figure 2. Bands [A-G] inclusive plotted against atomic mass units (amu). The best fit trend lines are constructed for the three isostructural carbonates.

Figure 3. NIR data plotted against the assigned overtone or combination derived from the additive sum of the MIR fundamentals data. Isostructural carbonate data points are shaded grey, [Li_2CO_3] and [Na_2CO_3] data points are plotted black. The wavenumber separation between the NIR data from each alkali is reported in brackets. Isostructural carbonate data points against which r^2 values are derived are shaded grey. **a)** NIR bands [A] (diamonds) , [B] (triangles) and [C] (circles) plotted against the corresponding M($3\nu_3$) value. **b)** Near-infrared bands [E] (diamonds) and [F] (triangles) plotted against the corresponding M($2\nu_1 + 2\nu_3$) combination wavenumber. Band [V] data point is marked with an open circle. **c)** NIR band [G] plotted against the corresponding M($\nu_1 + 3\nu_3$) combination wavenumber. **d)** NIR band [X] plotted against the corresponding M($2\nu_3 + 2\nu_4$) combination wavenumber.

Figure 4. Raman spectra of the alkali carbonates in the 100 - 300cm^{-1} wavenumber region of interest, y-axis is Raman intensity. NIR data giving the wavenumber difference with that of the MIR derived additive sum of the overtone or combination assignment are presented in square brackets giving the relevant band letter label and wavenumber total.

374 **Table 1**

Alkali carbonate	Int. mode ν_1 (cm^{-1}) Raman	Int. mode ν_2 (cm^{-1}) Infrared	Int. mode ν_3 (cm^{-1}) Infrared	Int. mode ν_4 (cm^{-1}) Infrared
$[Li_2CO_3]$	1092	865	1430	732 (741,723)
$[Na_2CO_3]$	1081 (1083 1079)	(886,880)	1419 (1425, 1413*)	697 (701,694)
$[K_2CO_3]$	1063	880	1400	686 (690,683)
$[Rb_2CO_3]$	1053	879	1380	684 (688,681)
$[Cs_2CO_3]$	1042	878	1367	676 (679, 674)

375

376

377 **Table 2**

	Band [A] (cm^{-1}) (2.359-2.458μm)	Band [B] (cm^{-1}) (2.321-2.416μm)	Band [C] (cm^{-1}) (2.226-2.339μm)	Band [D] (cm^{-1}) (2.174-2.227μm)	Band [E] (cm^{-1}) (2.004-2.102μm)	Band [F] (cm^{-1}) (2.004-2.102μm)	Band [G] (cm^{-1}) (1.969-1.881μm)
Li_2CO_3	4238	4308	4393	4506	4954	5049	5188
Na_2CO_3	4252	4345	4493	4599	4990	5080	5315
K_2CO_3	4234	4313	4407	4518	4996	5093	5205
Rb_2CO_3	4125	4194	4292	4490	4815	4996	5144
Cs_2CO_3	4067	4139	4275	4582	4757	4915	5078

378

379

Table 3

Assignment	($3\nu_3$)						($2\nu_1 + 2\nu_3$)				($\nu_1 + 3\nu_3$)		($2\nu_3 + 2\nu_4$)	
Band	[A]	L. mode	[B]	L. mode	[C]	L. mode	[E]	L. mode	[F]	L. mode	[G]	L. mode	[X]	L. mode
$[Li_2CO_3]$	52	-	18	-	103	97[a]	90	95[a]	5	-	194	194[a]	184	176,194[a]
$[Na_2CO_3]$	5	-	88	-	236	228[c]*	10	-	80	-	23	-	100	98[c]
$[K_2CO_3]$	34	-	113	109[b]*	207	201[b]*	70	76[a]	167	159,176[b]*	58	52[a]	45	52[a]
$[Rb_2CO_3]$	15	-	54	-	152	153[b]	51	-	130	132[b]	49	-	121	132[b]
$[Cs_2CO_3]$	34	43 [d]*	38	43 [d]*	174	170[d]	61	65[d]	97	72,114[d]	65	65[d]	No data	-

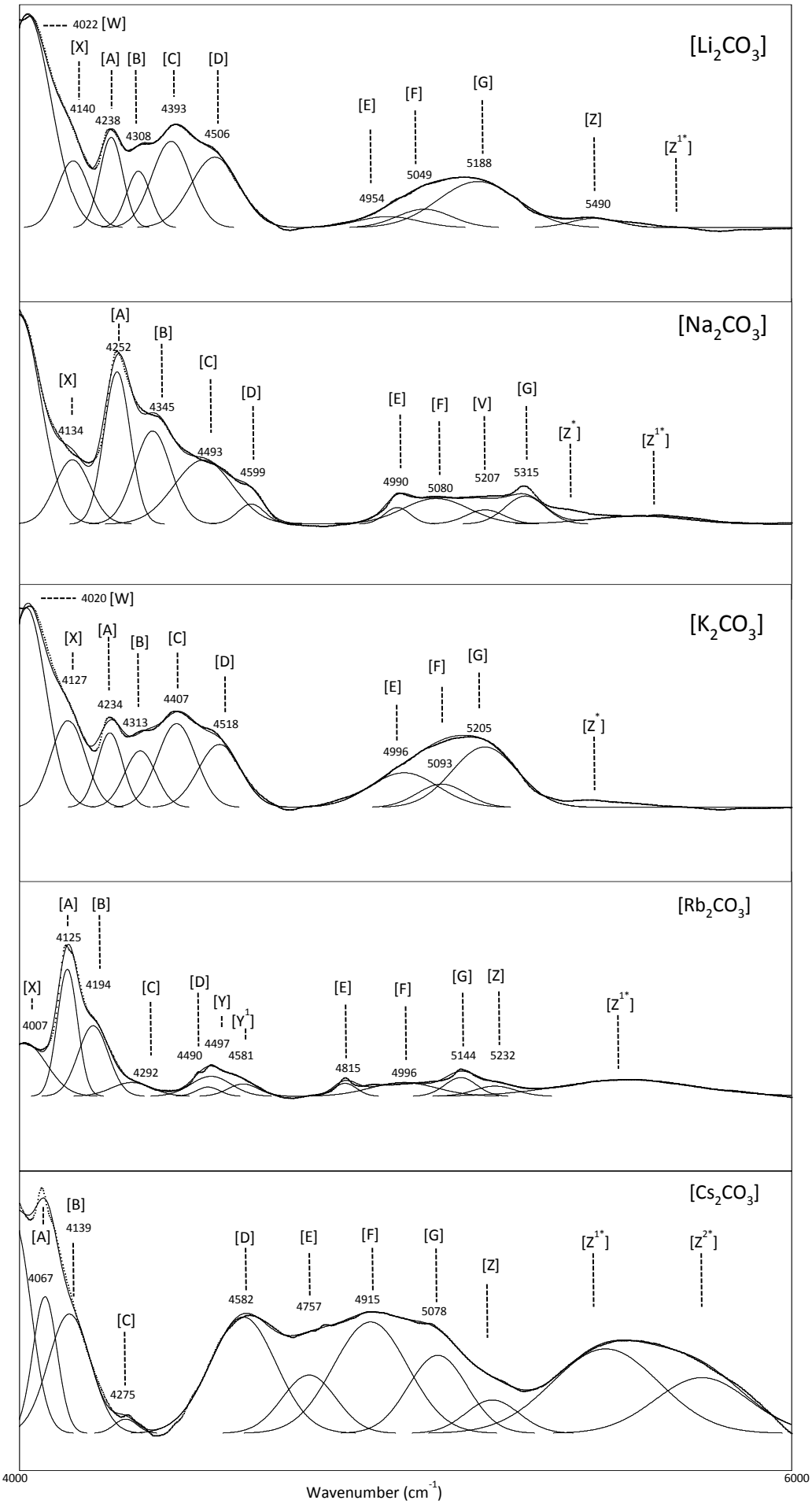
4022 [W]
[X]
[A]
[B]
[C]
[D]
[E]
[F]
[G]
[Z]
[Z1*]
4140
4238
4308
4393
4506
4954
5049
5188
5490
[Li2CO3]
[A]
[B]
[C]
[X]
[D]
[E]
[F]
[V]
[G]
[Z*]
[Z1*]
4252
4345
4134
4493
4599
4990
5080
5207
5315
[Na2CO3]
4020 [W]
[X]
[A]
[B]
[C]
[D]
[E]
[F]
[G]
[Z*]
4127
4234
4313
4407
4518
4996
5093
5205
[K2CO3]
[A]
[B]
[X]
[C]
[D]
[Y]
[Y1]
[E]
[F]
[G]
[Z]
[Z1*]
4125
4194
4007
4292
4490
4497
4581
4815
4996
5144
5232
[Rb2CO3]
[B]
[A]
[C]
[D]
[E]
[F]
[G]
[Z]
[Z1*]
[Z2*]
4139
4067
4275
4582
4757
4915
5078
[Cs2CO3]
4000
6000
Wavenumber (cm-1)

Figure 1

387 **Figure 2.**

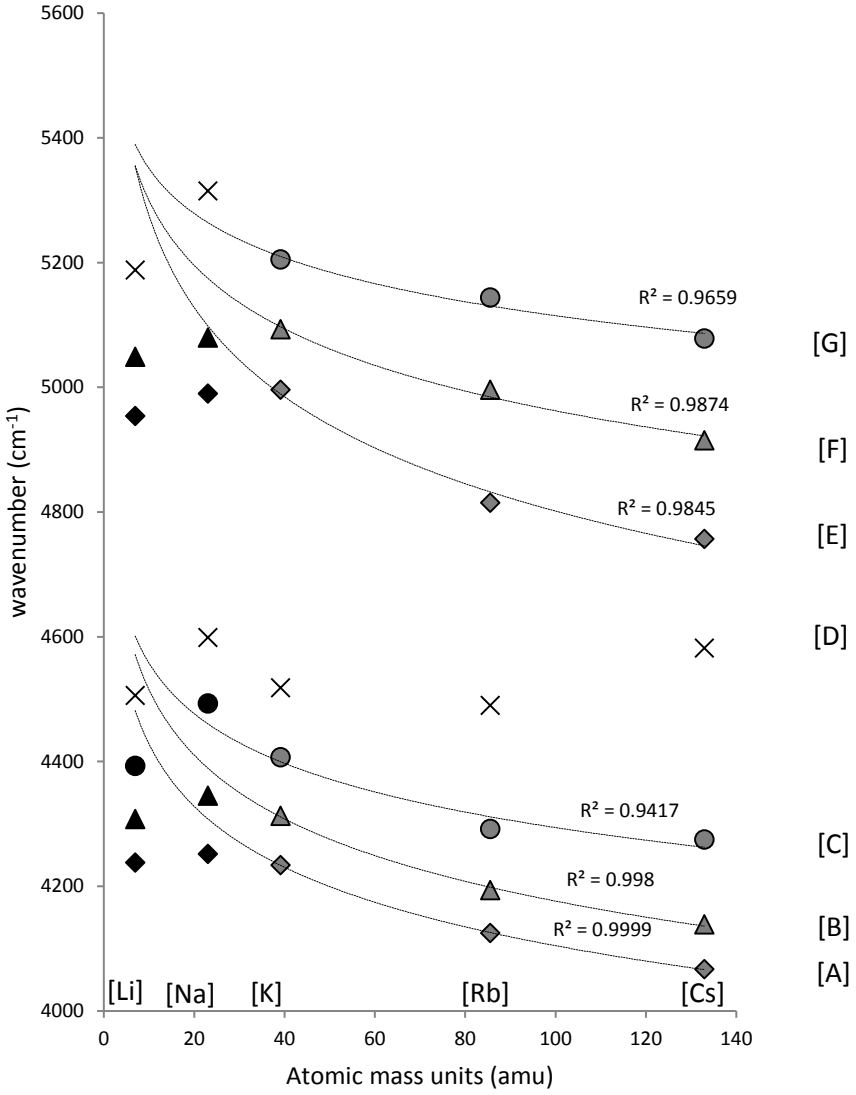

388

389

390

Figure 3

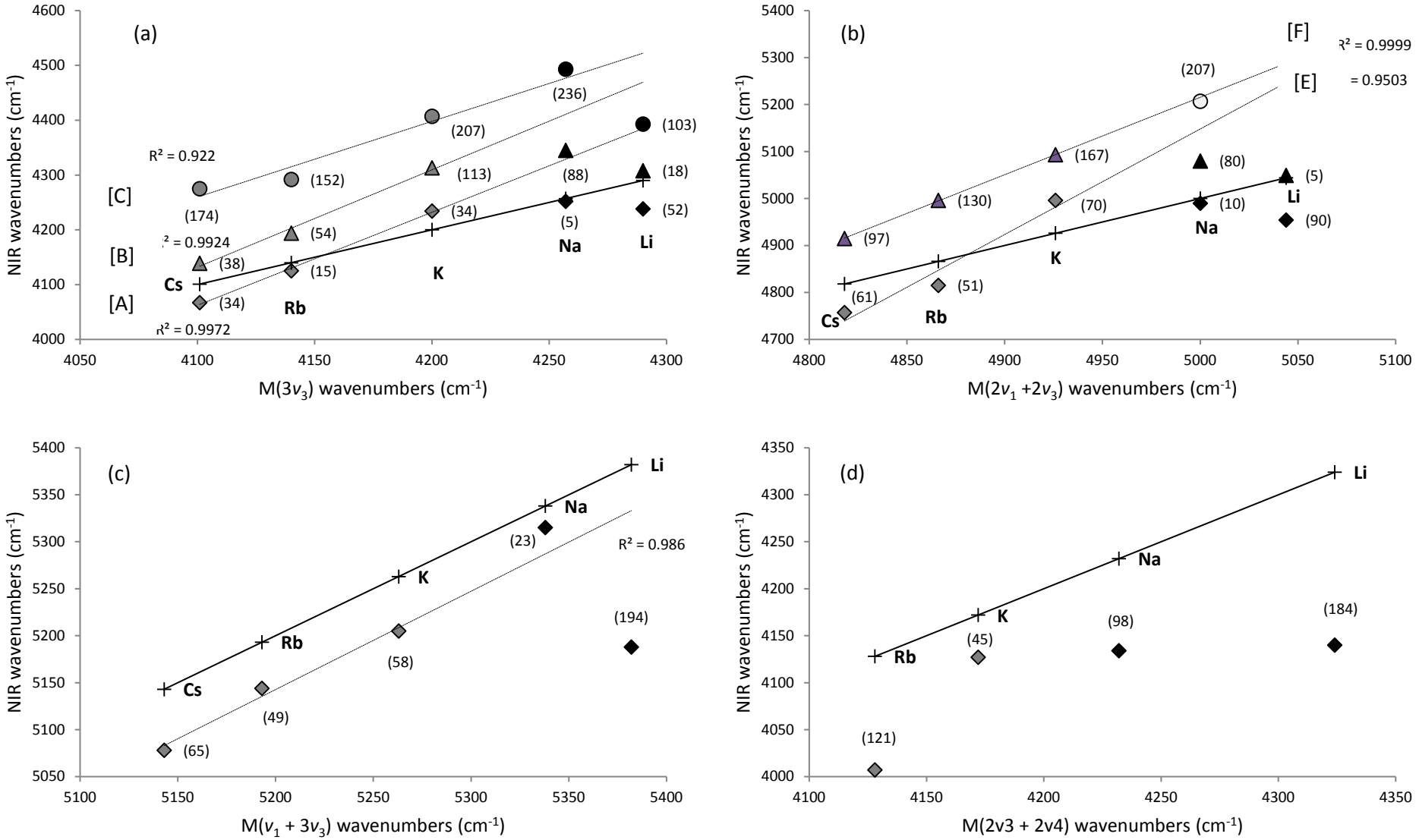
(a)
NIR wavenumbers (cm-1)
M(3ν3) wavenumbers (cm-1)
R² = 0.922
R² = 0.9924
R² = 0.9972
[C]
[B]
[A]
Cs
Rb
K
Na
Li
(b)
[F]
[E]
R² = 0.9999
= 0.9503
M(2ν1 +2ν3) wavenumbers (cm-1)
(c)
R² = 0.986
M(ν1 + 3ν3) wavenumbers (cm-1)
(d)
M(2v3 + 2v4) wavenumbers (cm-1)

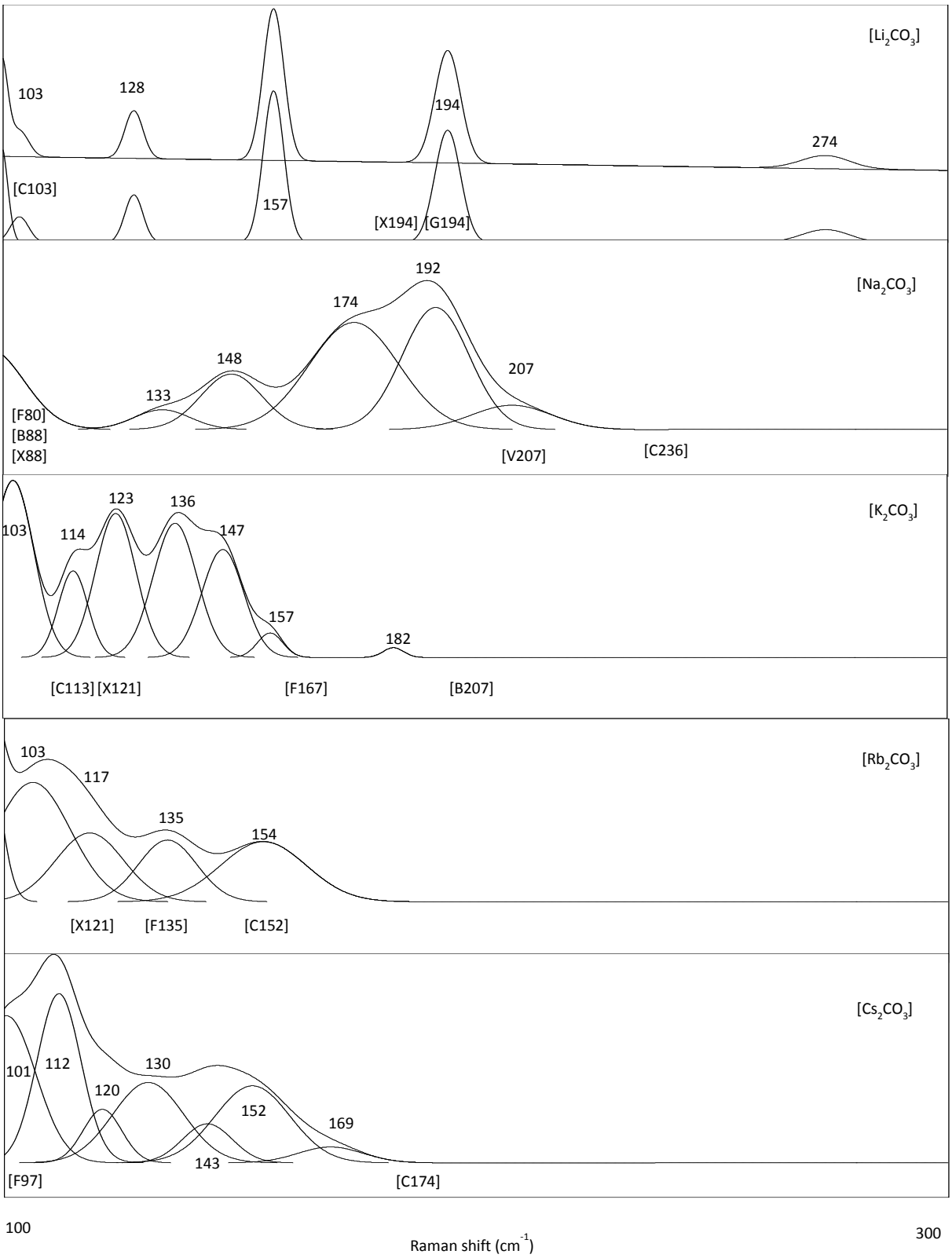
[Li2CO3]
103
128
194
274
[C103]
157
[X194]
[G194]
[Na2CO3]
192
174
148
207
133
[F80]
[B88]
[X88]
[V207]
[C236]
[K2CO3]
123
136
103
114
147
157
182
[C113]
[X121]
[F167]
[B207]
[Rb2CO3]
103
117
135
154
[X121]
[F135]
[C152]
[Cs2CO3]
101
112
130
120
152
169
143
[F97]
[C174]
100
300
Raman shift (cm-1)

Figure 4

395